Ionization of He, Ne, Ar, Kr, and Xe by proton impact: Single differential distributions in energy and angles

J. E. Miraglia

Instituto de Astronomía y Física del Espacio, Consejo Nacional de Investigaciones Científicas y Técnicas, and Departamento de Física, Facultad de Ciencias Exactas y Naturales, Universidad de Buenos Aires, Casilla de Correo 67, Sucursal 28, C1428EGA, Buenos Aires, Argentina

(Received 19 November 2008; published 26 February 2009)

In this paper we report energy and angular distributions of electrons emitted in collisions of protons with neon-(F^-,Ne^0,Na^+), argon-(Cl^-,Ar^0,K^+), krypton-(Br^-,Kr^0,Rb^+), and xenon-(I^-,Xe^0) isoelectronic series for high and intermediate impact energies. Calculations were performed within the continuum distorted wave-eikonal initial-state method using an angular expansion in spherical harmonics and a numerical evaluation of the radial functions corresponding to both: the initial (bound) and the final (continuum) states in the same central potential. The first Born approximation was calculated on equal footing. The shellwise local plasma approximation was also calculated when possible. A complete and exhaustive comparison with the available experimental data is carried out. We have spanned almost all the published experiments in our range of interest. Successes and failures of the different theoretical methods are pointed out. Possible signatures of many-electron effects are noticed.

DOI: 10.1103/PhysRevA.79.022708 PACS number(s): 34.50.Fa, 32.80.Aa, 33.15.Ry

I. INTRODUCTION

In a previous paper [1] (hereafter referred to as paper I) we undertook the task of calculating the ionization total cross section of protons colliding with elements of the helium (He^0,Li^+), neon (F^-,Ne^0,Na^+), argon (Cl^-,Ar^0,K^+), krypton (Br^-,Kr^0,Rb^+), and xenon (I^-,Xe^0) isoelectronic series. Although our particular interest focused on the electron yield as well as the total energy loss of protons impinging on NaCl-insulator surfaces at grazing angles, we also calculated ionization of rare gases (He, Ne, Ar, Kr, and Xe), where several experimental data are available. Calculations were performed within the continuum distorted wave-eikonal initial-state (CDW-EIS) method using an angular expansion in spherical harmonics and a numerical evaluation of the radial functions corresponding to both the initial (bound) and the final (continuum) states. The first Born approximation was also calculated on equal footing. For comparison, we also calculate the shellwise local plasma approximation (SLPA), which has been used to determine electron yields and energy loss of protons in collision with insulator surfaces [2]. Performances of the theoretical methods as compared with the experiments at level of total cross section were pointed out in paper I. For singly charged targets, we found that SLPA overestimates or underestimates the CDW-EIS depending whether the target is charged positive or negative.

In this paper we go on further and examine in detail energy and angle singly differential cross sections. Our target is to find in what energy and angle regions the theories fail by comparison with the measurements. For rare gases there is a series of experiments we can compare. In particular, for Ar targets, there are detailed experiments carried out in three different laboratories [3]. For Ne and Kr there are experiments of energy distributions in terms of the Platzman plot [4–6]. For Xe targets, there are few energy differential cross sections published by Toburen [7]. The article of Rudd *et al.* [6] collected all known experimental data on energy distributions at that time, and we compared with all of them in our range of energy. For angular distributions, on the contrary, there are very few data: we have only results for Ar [3]. We also report here the differential cross sections for charged targets since they are very relevant for collisions of protons with NaCl surfaces, but unfortunately, there are no experiments for negative and positive targets to compare with. Before proceeding, it should be mentioned that theoretical calculation within the CDW-EIS at level of double differential cross sections for He, Ne, and Ar was reported by Gulyás and Fainstein and collaborators using different potentials [8–12]. We will omit the target helium since there are several theoretical calculations; it has become lately an ideal benchmark to treat two active electron systems. In Sec. II we present the results and then the conclusions. Atomic units are used.

II. RESULTS

Before presenting the results, here is a brief description of the calculations. For each state, the central potential was determined from the Hartree-Fock wave functions and improved to achieve the best binding energy and moment of the position. As indicated in paper I, we expanded both the initial (bound) and final (continuum) electron wave functions in spherical harmonics times radial wave functions which require the numerical solution of the radial Schrödinger equation. To that end, we have used the code RADIALF developed by Salvat *et al.* [14]. The Clebsch-Gordan coefficients permit one to solve the angular coordinates in closed forms but radial functions need to be integrated numerically using a radial grid. With the use of the hypergeometric function ${}_2F_1$, which solves the integrals on the projectile variables, we obtain the T-matrix element $T(E,\Omega_E,\vec{\eta})$ for each electron energy (E), electron angle (Ω), and projectile transversal momentum transfer ($\vec{\eta}$). The double-differential cross section is obtained after integrating on $\vec{\eta}$, i.e.,

$$\frac{d\sigma_{nlm}}{dE\,d\Omega} = \frac{(2\pi)^4}{v^2}\int d\vec{\eta}|T_{nlm}(E,\Omega,\vec{\eta})|^2, \qquad (1)$$

where v is the projectile velocity and nlm are the usual quantum number of the initial state. In this paper we concentrate on the single differential cross sections, in energy and angle which read

$$\frac{d\sigma_{nlm}}{dE} = \int d\Omega \frac{d\sigma_{nlm}}{dE\,d\Omega}, \quad \frac{d\sigma_{nlm}}{d\Omega_E} = \int dE \frac{d\sigma_{nlm}}{dE\,d\Omega}. \qquad (2)$$

Total magnitudes, as displayed in this paper, involve the sum over all the relevant states of the target, i.e., on n, l, and m. The sum on n, l, and m was extended to include two complete shells: i.e., for Ne (nlm=$2p_{0\pm1}$, $2s$, and $1s$), Ar ($3p_{0\pm1}$, $3s$, $2p_{0\pm1}$, and $2s$), Kr ($4p_{0\pm1}$, $4s$, $3d_{0\pm1\pm2}$, $3p_{0\pm1}$, and $3s$), and Xe ($5p_{0\pm1}$, $5s$, $4d_{0\pm1\pm2}$, $4p_{0\pm1}$, and $4s$). For impact energies larger than 1 MeV, we have concentrated on the calculation of the Born approximation with a more accurate numerical precision. In these cases, we use 28 ejection angles, up to 50 electron energies, and up to $l_{\max}$=32. For further details of the calculations, see paper I.

A. Energy distributions

We start by studying the Ar target, following on the article of Rudd *et al.* [3], who reported an exhaustive set of experimental double differential cross sections by protons in our range of interest. To our interest, the authors also reported single differential cross sections integrated in either angle or energy performed in three different laboratories. In Fig. 1 we plot the CDW-EIS (solid lines), Born approximation (dotted lines), and SLPA (dashed lines) along with the measured cross sections. For 50 keV we have two sets of experiments, and for 300 keV we have the convergence of the measurements coming from the three laboratories involved in the project. In general, the theories have a reasonable performance running close to the experiments along six orders of magnitude. However, on closer examination, two disagreements are observed.

(i) First, the CDW-EIS does not reproduce the experiments in the low-electron-energy regime. This discrepancy has been also observed in Ref. [9] at the level of double differential cross section and no explanation was found. Later on Kirchner *et al.* [12] demonstrated that the energy distribution depends strongly on the explicit form of the local static exchange potential. The authors used the optimized potential model (OPM) and obtained a better agreement with the experiments. Our V_{3p} potential agrees perfectly well with the OPM one in the range plotted in Fig. 1 of Ref. [12]. But our V_{3s} potential is substantially smaller than the OPM in the same range. We have compared our wave functions with the ones obtained using the OPM calculated with the program of Ref. [13] and verify that they are indistinguishable from each other. Unexpectedly, the SLPA shows a good agreement with the experiments in that low-energy region. It is known that the SLPA is a first-order model which considers the target as a local free-electron gas. The success of this model is the description of the total stopping power and straggling. We cannot expect, however, the SLPA to account for the details

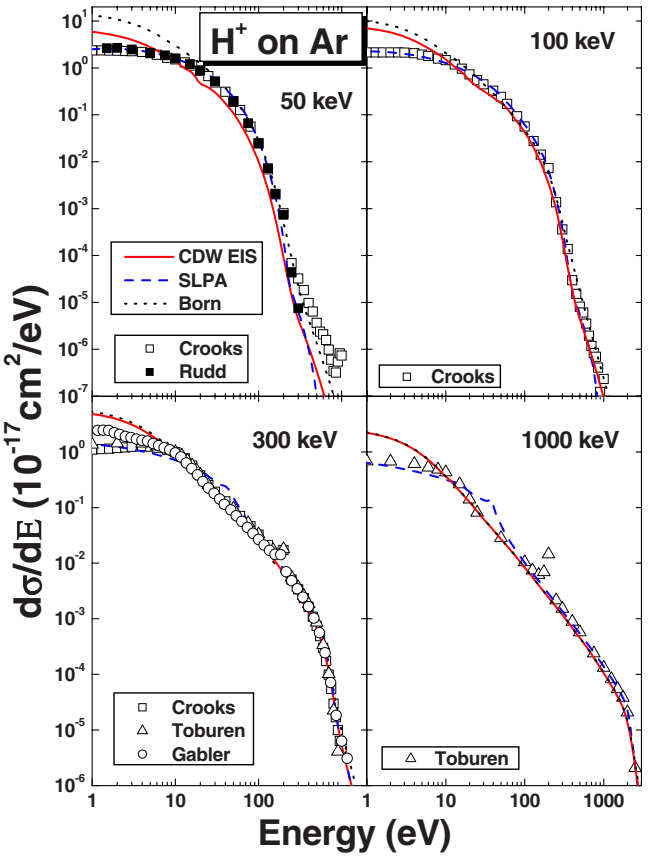

FIG. 1. (Color online) Energy differential cross sections for ionization of Ar by protons at four different impact energies as indicated. Symbols (green), experiments reported by Rudd *et al.* [3]. The different symbols correspond to different laboratories as indicated in the same reference. Crooks and Rudd, and Rudd performed at Bethlen; measured by Toburen at Battelle, and Gabler and Stolterfoht at Hahn-Meitner, Germany. Theories: Solid (red) lines, CDW-EIS; dotted (black) lines, Born approximation; and dashed (blue) lines, SLPA.

of the energy distribution. Instead, the CDW-EIS is expected to be a more specialized theory to that end. It is nonlinear which means that it accounts for higher order in the projectile charge, including the capture to the continuum, and its calculation is quite rigorous. Anyway, even with these limitations, the SLPA accounts for a many-electron system and explains the low-energy electron regime. Having this point in mind, we essay possible explanations for these low-energy behaviors as explained next.

The CDW-EIS is a theory based on the *independent electron* model, in which electrons not involved in the transitions are considered frozen. On the other hand, the SLPA considers all the electrons of a given shell fully *correlated* within the Lindhard-Louis-Levine dielectric-response function. It would be more convenient to classify it as an *independent shell* approximation since all the electrons of the shell react self-consistently to the presence of the projectile. Electrons emitted with low energies essentially stem from large distances from the projectile seeing the projectile *shielded* by the other electrons, and therefore their Coulomb charge diminishes. In consequence, the differential cross section

should be smaller as observed in the experiments, and in agreement with the SLPA prediction. If this were the case, and this is to be proven, we would be in the presence of a *many-electron* signature and it would open an interesting field to explore. There could be another source involving a many-electron process—the polarization potential created by the remaining electrons upon the emitted one—but as we are dealing with Coulomb potentials this effect should not be noticeable. There are experimental difficulties to determine accurately differential cross sections for slow ejected electrons, say $E<10$ eV [7], so the development of a theory that can predict an accurate energy distribution can serve not only as a valuable tool to gauge experimental errors [3] but also to determine the physics involved in large distances (soft) collisions. This would be of particular interest in collision with solids where the interactions are diminished by the presence of the remaining bulk. There is another possibility left: there is not a many-electron effect, the agreement of the SLPA is fortuitous, and the CDW-EIS simply fails to describe the soft peak in our range of velocities. At large electron energies both the CDW-EIS and SLPA converge to the Born approximation. This convergence is to be expected since high-energy electrons come from head-on collisions (short distances) where the nucleus projectile charge is mandatory.

(ii) The second outcome to be noted is that at large proton energies, the SLPA distribution starts to show a spurious peak at around 40 eV, not present in the experiments. This structure can be attributed to a local or quasiplasmon effect as explained next. The basic assumption of the local plasma approximation is to consider that at every position, the projectile samples a free-electron gas with a plasmon energy $\omega_p=\sqrt{4\pi n(r)}$, where $n(r)$ is the local electronic density. To visualize the problem, it is convenient to change the integration variable. Instead of sampling all the projectile positions r, we can integrate on the all possible plasmon energies ω_p. The change of variable reads [15,16]

$$dr=\frac{\omega_p\, d\omega_p}{2\pi}\frac{1}{\left(\frac{dn(r)}{dr}\right)}. \tag{3}$$

It becomes clear that for the energy values so that $dn(r)/dr=0$, the denominator of Eq. (3) diverges and that divergence is called "pseudo" plasmon here. Mathematically, this divergence has generally a logarithmic structure and it is integrable. For a homogenous free-electron gas, the electronic density is a constant in every position and all the derivatives of the density are zero, and therefore we find a Lorentzian-type peak which is the signature of "real" plasmon. Thus we can think that a real plasmon comes into existence when the cancellation of the successive derivatives of the electron density allows a constant value for the density in the whole space. As the velocity increases, the pseudoplasmons appear producing unrealistic structures and they should be considered as an artifact of the theory.

The energy distributions present a scale involving several orders of magnitudes and so the fine details could pass unnoticed. An alternative way to plot the energy distribution is the Platzman plot whose physical interpretation is the effective number of electrons. This is a ratio between $d\sigma/dE$ and the "modified" Rutherford cross section by impact of one electron with the same energy. It reads

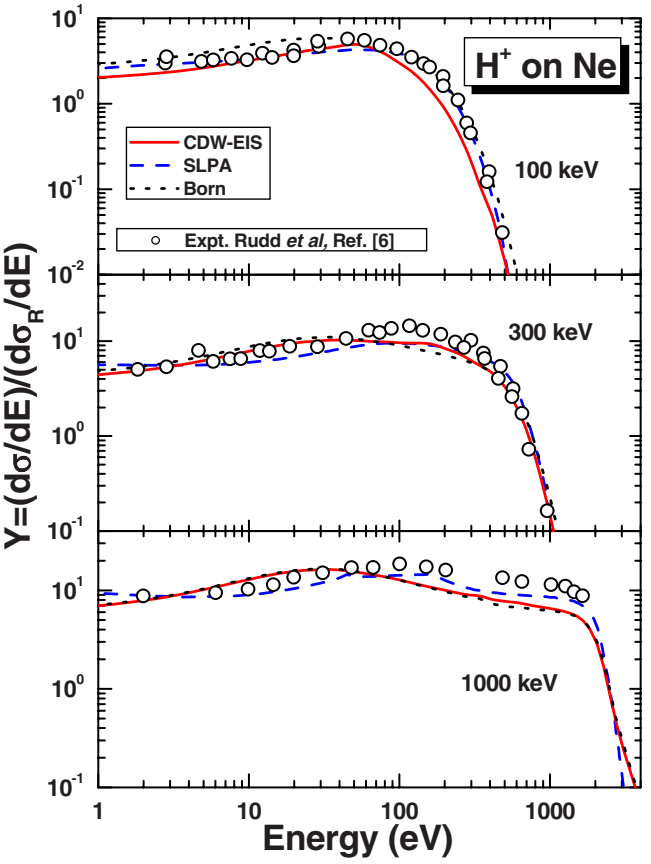

FIG. 2. (Color online) Platzman plot from protons on neon as a function of the emitted electron energy in electron volts for three impact energies. Empty circles (green), experiments from Crooks and Rudd [21], digitalized from Rudd *et al.* [6]. Lines, theories as in Fig. 1.

$$Y=\frac{d\sigma/dE}{(d\sigma/dE)_{\mathrm{Rud}}}=\frac{v^2(E+I)^2}{4\pi}\frac{d\sigma}{dE}, \tag{4}$$

where I is the modulus of the binding energy of the outermost shell. The difference between the modified Rutherford expression and the "original" one is the presence of I. For the rare gases we used the values of Bunge *et al.* [17] ($I=0.850$, 0.591, 0.524, and 0.457 a.u. for Ne, Ar, Kr, and Xe, respectively). The magnitude Y is a powerful tool for analyzing and identifying the different features in the SDCS in fine detail [5,6].

In Fig. 2 we present the theoretical Platzman plots for Ne and compare with the experiments [6]. The agreement of the theory with the experiments is satisfactory and it also agrees with the results obtained with the OPM as reported in Fig. 2(a) of Ref. [12]. In this case our theory runs along the experiment at low electron energies. For 1-MeV protons, the deficiency of the CDW-EIS and Born approximation at very large electron energy, where the differential cross section falls off four orders of magnitude, may be possibly due to the insufficient number of angular momentum used. The good

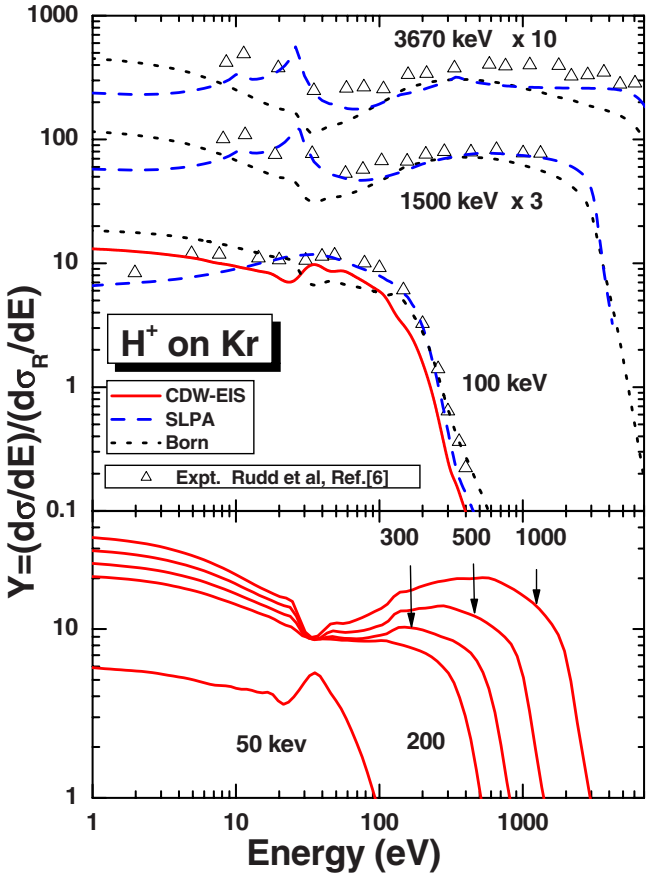

FIG. 3. (Color online) (Upper figure) Platzman plots from protons on krypton as a function of the emitted electron energy in electron volts. Empty triangles (green), experiments from Toburen *et al.* [5], digitalized from Rudd *et al.* [6]. Lines, theories as in Fig. 1. (Lower figure) Platzman plots in CDW-EIS approximation for the same target but for different impact energies.

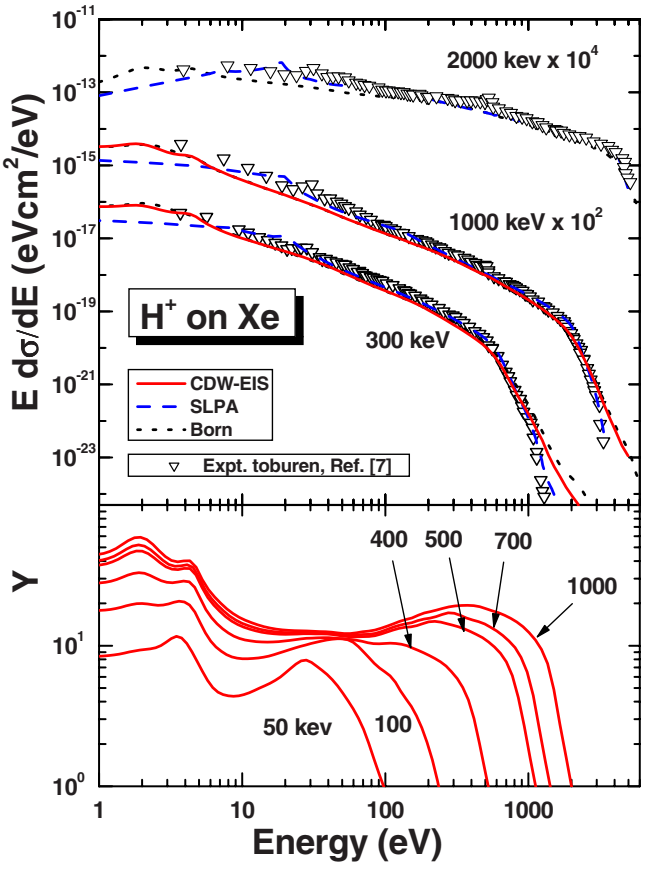

FIG. 4. (Color online) (Upper figure) Energy differential cross sections multiplied by the electron energy for ionization of xenon by impact of protons. Empty triangles (green)—experiments from Toburen Ref. [7]. Theories, as in Fig. 1. (Lower figure) Platzman plots in CDW-EIS approximation for the same target but for different impact energies.

agreement at 100-keV impact energy may be fortuitous, as pointed out in Ref. [5] where also the first Born calculations using Hartree-Fock wave functions were presented. This good agreement at 100-keV is not supported by the convergence at higher impact energy, as one should expect. The SLPA gives also a good account of Y but, for 1 MeV it starts to present a pseudoplasmon at 180 eV.

Platzman plots for krypton are presented in Fig. 3 and compared with experimental data for three impinging energies: to our knowledge, the only available in our range of energies. For 1- and 3.67-MeV impact energies, we display just the Born approximation because the CDW-EIS is almost identical. The dip at around 30 eV is noteworthy. The dip is also notable in the experiment but much less dramatic than the theory. In the lower part of the figure, we also present some theoretical prediction of Y in the CDW-EIS for other energies to have a more complete idea of shape and position of the dip. To be sure that the dip is not rooted in a numerical problem, we carried out the calculation with the Born approximation with 28 ejection angles, 50 electron energies, and up to $l_{max}=32$. Although this dip occurs when the electron initial wave function has nodes, it would not be appropriate to identify it fully with Cooper minima. It would be better to say that it occurs as a consequence of the nodes of the Fourier transform of the outer $4p \pm 1$ states. As the squared modulus of the Fourier transform gives the probabil-

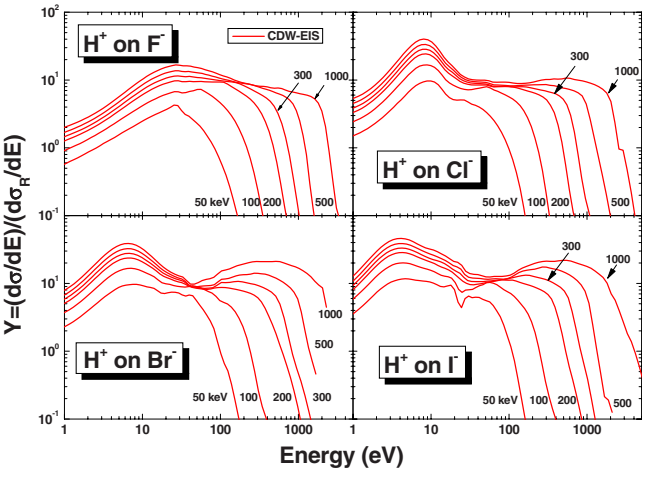

FIG. 5. (Color online) Platzman plot calculated with the CDW-EIS for protons on negative charged ions at different impact energies as a function of the ejected electron energy in electron volts.

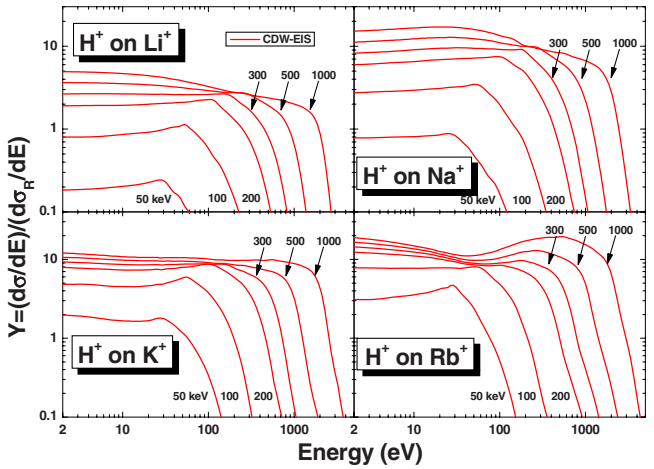

FIG. 6. (Color online) Platzman plot calculated with the CDW-EIS for protons on positive charged ions at different impact energies as a function of the ejected electron energy in electron volts.

ity of the state having the electron a given velocity, we can explain the dip as related to the incapability of the state to provide electrons with velocities so that a binary collision with the projectile would end in the energy region of the dip. The theoretical dip is quite significant and this energy region should be explored more carefully. At 100 eV the CDW-EIS again does not reproduce the experiments in the low-electron-energy regime.

In Fig. 4 we display energy distributions times the electron energy for three different proton velocities: 300, 1000, and 2000 keV on xenon targets. Our theoretical results CDW-EIS, Born approximation, and SLPA are compared with the experiments published by Toburen [7], the only ones to our knowledge. In general all the theories work reasonably well: they describe the experiments along 6 orders of magnitudes. It is not clear whether the experiments follow the CDW-EIS approximation in the low-energy regime. Again for large velocities the SLPA presents a pseudoplasmon at 20 eV. It corresponds to a maximum of the density of the $5p$-Xe state at 0.65 a.u. from the nucleus [18]. Peaks occurring in the experiments at 30–40 and 400–500 eV correspond to Auger transitions filling the vacancies in the N and M shells. In the lower part we display Y plots for different energies. Here one can identify better the fine structures of the distributions. The waves of Y should be adjudicated to the nodes of the Fourier transform of the outer $5p \pm 1$ and in a lesser scale to the inner shells.

In Figs. 5 and 6 we report the Platzman ratio Y for charged ions. For negative and positive ions we used the values of I given by Clementi and Roetti [19] (I=0.180, 0.150, 0.138, and 0.129 for F^-, Cl^-, Br^-, and I^-; and I =2.79, 1.79, 1.17, and 1.01 for Li^+, Na^+, K^+, and Rb^+, respectively). It can be observed that positive ions do not present any structure at all, but negative ones do exhibit interesting structures mainly because of the outer shells which are relevant in this range of energy. Although less noticeable,

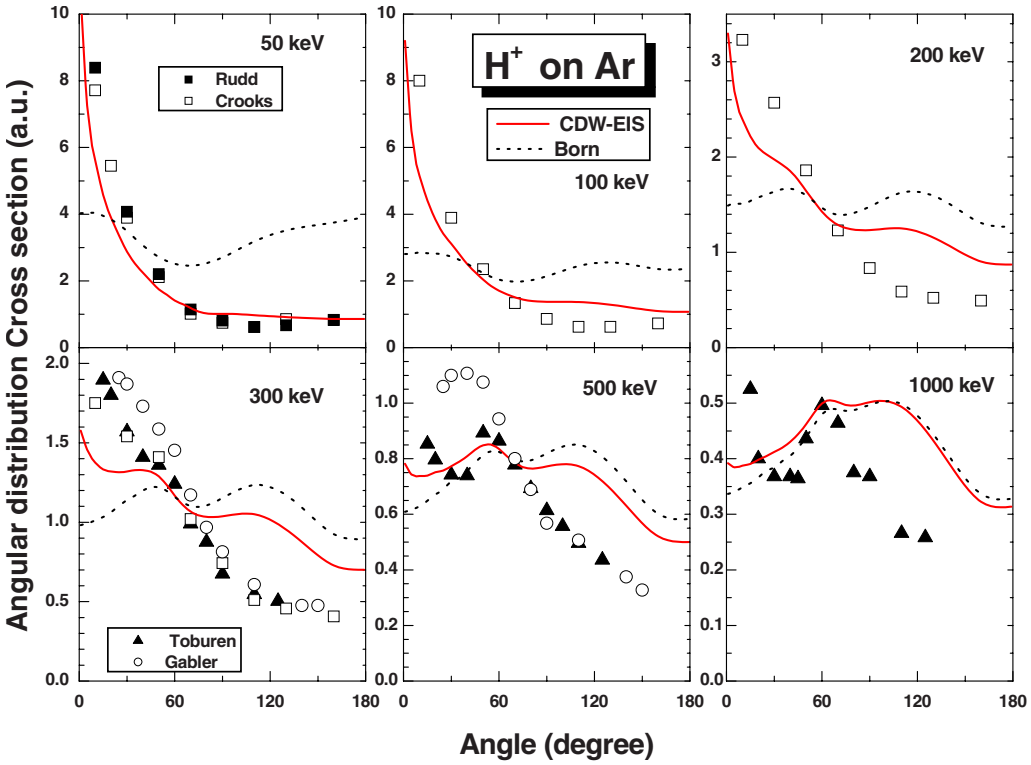

FIG. 7. (Color online) Angular differential cross sections for ionization of Ar by protons at six different impact energies as indicated. Symbols (green), experiments reported by Rudd *et al.* [3]. The different symbols correspond to different laboratories as indicated in the same reference. Crooks and Rudd, and Rudd performed at Bethlen; Toburen measured at Battelle, and Gabler and Stolterfoht at Hahn-Meitner, Germany. Theories: Solid (red) lines, CDW-EIS; dotted (black) lines, Born approximation. This latter approximation is plotted only for 300 and 1000 keV.

it is possible to observe a dip minimum in Br^-, probably as a consequence of belonging to the Kr isoelectronic series; it seems to be the most sensitive one. To our knowledge there is no single differential cross section published for charged targets in our range of interest. Knowing these distributions plays a very important role in the prediction of spectra of the emitted electrons in collisions of protons with insulators.

B. Angular distributions

We start again with argon where angular single differential measurements were published in detail in Ref. [3]. Figure 7 presents angular distributions for six proton impact energies. CDW-EIS and Born approximation are also plotted. The SLPA is not shown since it cannot provide information on the direction of the ejected electron; it does not account for the target nucleus recoil which is important in this case. At the lower impact energies large differences are observed between the CDW-EIS and the Born approximation mainly in the forward direction and should be attributed to the capture into the continuum processes. As the proton energy increases both theories converge, but not to the extent of the experiments at large angles. The data run quite below the present theories, even at 1 MeV, where one should expect the Born approximation to converge to the data. At 1-MeV proton energy, the recommended experimental value for the total cross section is 5.07 a.u [20], which compares reasonably well with 5.90 predicted by the CDW-EIS [1], that is 16% above [21–25]. However at the largest angle measured (125°) the theories run 70% above, which is a serious disagreement to take into consideration. We should also keep in mind that the experiments include the Auger emission. These postcollisional processes will increase the theoretical values at larger angles even more since the decay electrons present isotropiclike spectra.

In Fig. 8, we display angular distributions of protons for the rest of the rare gases, i.e., Ne, Kr, and Xe. We also include He for completeness, although this system has been studied in detail by other authors within the Born approximation and CDW-EIS at the level of double differential in detail in Ref. [26,27]. Along the CDW-EIS, the Born approximation is included for all the cases but for just two energies: 300 keV, i.e., the minimum impact energy for which it converges to the CDW-EIS at level of total cross section, and 1 MeV, the maximum energy here studied. Note that, although at 300 keV the total cross section in Born approximation is closed to the CDW-EISA, there are still substantial differences at the level of angular distribution due to the capture into the continuum mechanism. As pointed out by Toburen [7], there is an enhancement of cross sections for electron emission into larger angles for the heavier targets. As the velocity increases the angular distributions are ruled by low-energy electrons which are ejected in soft collisions at large impact parameters, and as a consequence of the dipole transition rules one would expect the distribution to be more isotropic as observed in the experiments for all the targets. Unfortunately no angular distributions were reported for Ne, Kr, or Xe.

Finally in Figs. 9 and 10, we display angular distributions for impact of protons on negative and positive target ions

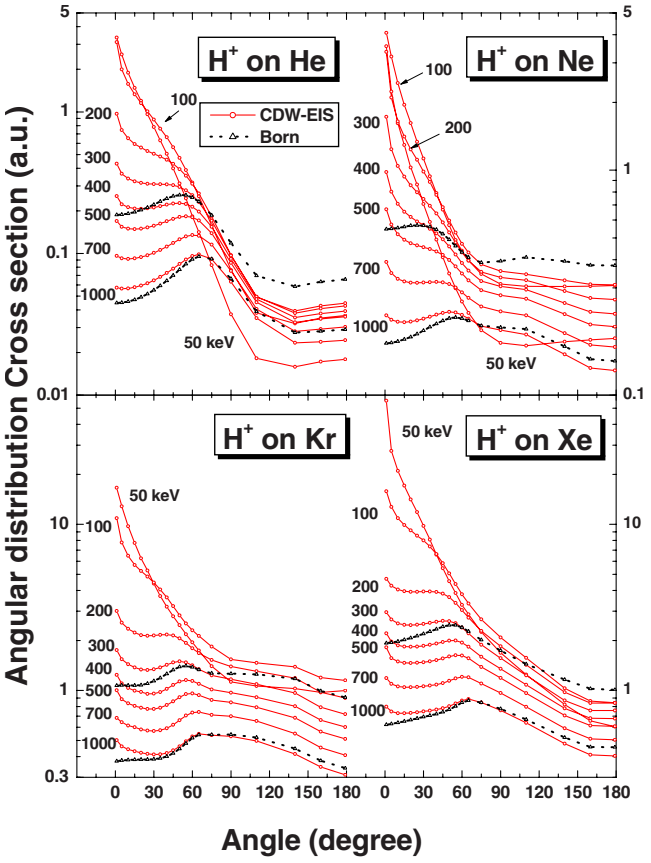

FIG. 8. (Color online) Angular differential cross section for ionization of rare gases by protons at different impact energies as indicated. Theories: Solid (red) lines, CDW-EIS; dotted (black) lines, Born approximation. This latter approximation is plotted only for 300 and 1000 keV.

where the same features are observed. Inspecting these figures, one could say that negative ions provide more isotropic distributions than the ones of positive targets. No experiments have been reported for these cases yet.

III. CONCLUSIONS

Single differential cross sections in energy and angle for protons on rare gases and singly charged ions have been reported in detail. Theoretical methods CDW-EIS and first Born approximation were presented and compared with almost all the experimental data available in the high-energy regime, i.e., between 50 keV and few MeV. A complete set of results is plotted which will help to understand future experiments. For energy distributions SLPA results were also displayed. The comparison was designed to be as complete, comprehensive, and exhaustive as possible.

We can summarize the following points:

(i) At level of energy distribution, the CDW-EIS and first Born approximation give in general good account of the available experiments in the high-electron energy range.

(ii) Surprisingly the SLPA gives a very good agreement with the experiments except at some specific emission energies where the derivative of the electronic density cancels,

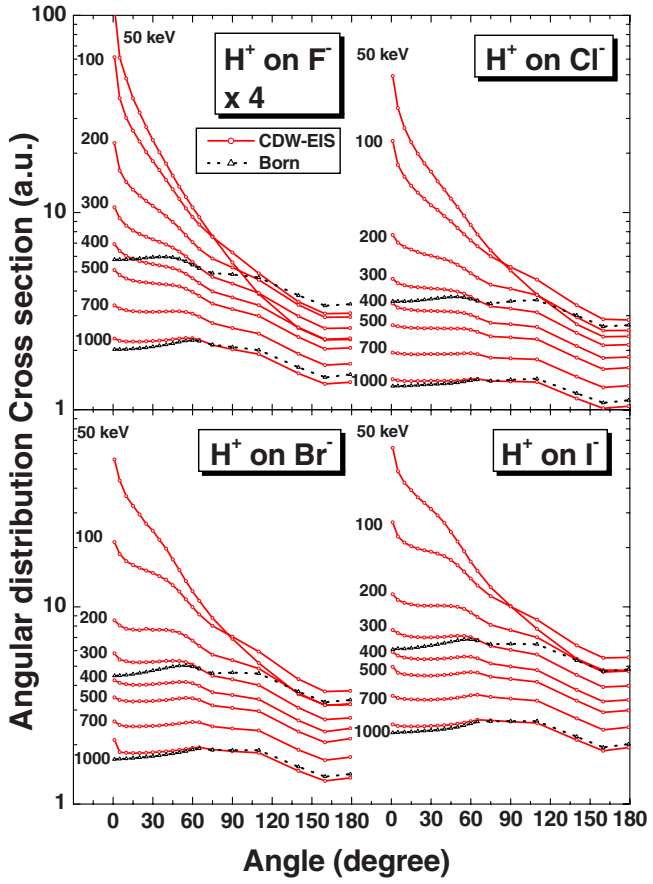

FIG. 9. (Color online) Angular differential cross section for ionization of negative ions by protons at different impact energies as indicated. Theories: Solid (red) lines, CDW-EIS; dotted (black) lines, Born approximation. This latter approximation is plotted only for 300 and 1000 keV.

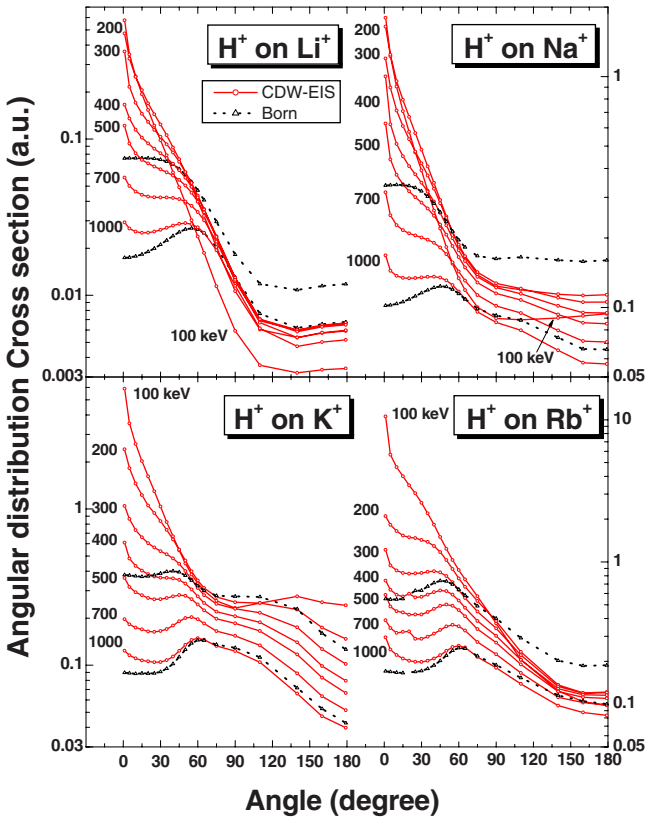

FIG. 10. (Color online) Angular differential cross section for ionization of positive ions by protons at different impact energies as indicated. Theories: Solid (red) lines, CDW-EIS; dotted (black) lines, Born approximation. This latter approximation is plotted only for 300 and 1000 keV.

giving rise to spurious pseudoplasmons (only at very large impact energies).

(iii) There is an overestimation of our CDW-EIS calculations for Ar at low electron energy. It would be interesting to study if there is a deficiency of the static potential used in this work, or in the presence of correlated processes at an impact velocity range where the single-electron model is expected to work. For the other rare gases, the CDW-EIS seems to work properly at least at level of energy distribution.

(iv) At level of angular distribution, the performance of our CDW-EIS method for argon is disappointing. At large impact velocities where one would expect this method to converge both to the Born approximation and to the experiments, they do not. Our calculations are consistently large at large angles where we have up to 70% of difference with the experiment.

It would be interesting to have measurements of single differential cross sections at low electron energy to investigate the role of the potential and the possibility that a new physics is involved that is not accounted for by the CDW-EIS approximation.

ACKNOWLEDGMENTS

The authors would like to acknowledge financial support from CONICET, UBACyT, and ANPCyT of Argentina.

[1] J. E. Miraglia and M. S. Gravielle, Phys. Rev. A **78**, 052705 (2008).
[2] A. J. García and J. E. Miraglia, Phys. Rev. A **74**, 012902 (2006); **75**, 042904 (2007).
[3] M. E. Rudd, L. H. Toburen, and N. Stolterfoht, At. Data Nucl. Data Tables **23**, 405 (1979).
[4] W.-Q. Cheng, M. E. Rudd, and Y.-Y. Hsu, Phys. Rev. A **39**, 2359 (1989).
[5] L. H. Toburen, S. T. Manson, and Y.-K. Kim, Phys. Rev. A **17**, 148 (1978).
[6] M. E. Rudd, Y.-K. Kim, D. H. Madison, and T. Gay, Rev. Mod. Phys. **64**, 441 (1992).
[7] L. H. Toburen, Phys. Rev. A **9**, 2505 (1974).
[8] P. D. Fainstein, R. D. Rivarola, and V. H. Ponce, J. Phys. B **21**,

287 (1988), and references within.
[9] L. Gulyás, P. D. Fainstein, and A. Salin, J. Phys. B **28**, 245 (1995).
[10] L. Gulyás and T. Kirchner, Phys. Rev. A **70**, 022704 (2004).
[11] L. Gulyás and P. D. Fainstein, J. Phys. B **31**, 3297 (1998).
[12] T. Kirchner, L. Gulyás, H. J. Lüdde, E. Engel, and R. M. Dreizler, Phys. Rev. A **58**, 2063 (1998).
[13] J. D. Talman, Comput. Phys. Commun. **54**, 85 (1989).
[14] F. Salvat, J. M. Fernández-Varea, and W. Williamson, Jr., Comput. Phys. Commun. **90**, 151 (1995).
[15] W. Brandt and S. Lundqvist, Phys. Rev. **139**, A612 (1965); see Eq. (36).
[16] R. E. Johnson and M. Inokuti, Comments At. Mol. Phys. **14**, 19 (1983).
[17] C. F. Bunge, J. A. Barrientos, and A. V. Bunge, At. Data Nucl. Data Tables **53**, 113 (1993).
[18] It is interesting to recall the photoionization of 4*d* Xe presents a maximum at 100 eV [D. L. Ederer, Phys. Rev. Lett. **13**, 760 (1964)] and it is adjudicated to collective response of the shell electrons.
[19] E. Clementi and C. Roetti, At. Data Nucl. Data Tables **14**, 177 (1974).
[20] M. E. Rudd, Y.-K. Kim, D. H. Madison, and J. W. Gallagher, Rev. Mod. Phys. **57**, 965 (1985).
[21] J. B. Crooks and M. E. Rudd, Phys. Rev. A **3**, 1628 (1971).
[22] T. L. Criswell, L. H. Toburen, and M. E. Rudd, Phys. Rev. A **16**, 508 (1977).
[23] J. W. Hooper, D. S. Harmer, D. W. Martin, and E. W. McDaniel, Phys. Rev. **125**, 2000 (1962).
[24] L. I. Pivovar and Yu. Z. Levchenko, Sov. Phys. JETP **25**, 27 (1967).
[25] The experimental recommended value in Ref. [20] is 5.07 ± 0.50 a.u. Other experiments of proton on Ar at 1 MeV give similar values, for example, Ref. [5] reports 4.39 ± 0.85, Ref. [23] reports 5.57 ± 0.32, and Ref. [24] reports 4.57 ± 0.46.
[26] S. T. Manson, L. H. Toburen, D. H. Madison, and N. Stotelfoht, Phys. Rev. A **12**, 60 (1975).
[27] M. E. Rudd, L. H. Toburen, and N. Stolterfoht, At. Data Nucl. Data Tables **18**, 413 (1976).